JACS
JOURNAL OF THE AMERICAN CHEMICAL SOCIETY

Communication

pubs.acs.org/JACS

# Porous Field-Effect Transistors Based on a Semiconductive Metal–Organic Framework

Guodong Wu,[†,§] Jiahong Huang,[†,‡,§] Ying Zang,[†] Jun He,[*,‡] and Gang Xu[*,†]

[†]State Key Laboratory of Structural Chemistry, Fujian Institute of Research on the Structure of Matter, Chinese Academy of Sciences, Fuzhou, Fujian 350002, China

[‡]School of Chemical Engineering and Light Industry, Guangdong University of Technology, Guangzhou, Guangdong 510006, China

Supporting Information

**ABSTRACT:** Recently, the emergence of conductive metal–organic frameworks (MOFs) has given great prospects for their applications as active materials in electronic devices. In this work, a high-quality, free-standing conductive MOF membrane was prepared by an air–liquid interfacial growth method. Accordingly, field-effect transistors (FETs) possessing a crystalline microporous MOF channel layer were successfully fabricated for the first time. The porous FETs exhibited p-type behavior, distinguishable on/off ratios, and excellent field-effect hole mobilities as high as 48.6 $cm^2\ V^{-1}\ s^{-1}$, which is even comparable to the highest value reported for solution-processed organic or inorganic FETs.

Metal–organic frameworks (MOFs) are a class of crystalline nanoporous materials in which inorganic building units are connected by organic linkers via coordination bonding.[1] Over the past few years, material chemists have used MOFs for their potential applications mainly in gas storage, gas separation, and catalysis.[2] Recently there has been a growing interest in studying MOFs as a new type of semiconducting materials. MOFs with conductivity higher than 0.1 S $cm^{-1}$ have been achieved by Allendorf, Dincă, Nishihara, and others.[3] Talin and co-workers presented the first example of a thermoelectric effect in TCNQ@$Cu_3(BTC)_2$ with a large positive Seebeck coefficient.[4] Grzybowski, Li, and Liu reported the potential storage of electrical information in MOF-based memory devices.[5] Dincă et al. used a conductive MOF, $Cu_3(HITP)_2$, to fabricate chemiresistive sensor devices.[6] These pioneering scientific reports have set the foundation for the application of MOFs within the domain of electronic devices.

Field-effect transistors (FETs) are three-terminal semiconductor devices where a voltage related to the "gate" terminal controls the electric current in the channel between the "source" and the "drain" terminals. FETs play critical roles in modern electronic applications.[7] For example, they are well-known as the fundamental building blocks of the central processing unit (CPU) in computers. More recently, their versatile features have expanded their applications to state-of-the-art technologies including flat panel displays, memory devices, sensors, nanofluidic transistors, etc.[8] Moreover, a FET presents a powerful way to investige the intrinsic electronic properties of semiconducting materials. The charge carrier type, carrier mobility, and carrier concentration can be revealed by using the semiconductor as the channel material in the device.[9] The features of conductive MOFs, such as long-range crystallinity, rich and designable structure, modulatable pathways for charge transport, tunable electronic band structure by ligand modification and metal selection, ultralight and low density, and easy solution processability for membrane preparation make them very attractive for use as active channel materials in FETs.[10] On the other hand, FETs with porous channels can greatly extend their applications on voltage-gated ion channels/microfluidic chips and vastly enhance the sensitivity of FET-based gas/ion sensors.[11] FETs with meso- or macroporous channels (ranging from several nanometers to hundreds of nanometers) have been reported.[12,13] However, they normally present large size-distributed and disorderly arranged pores. Recently, FETs based on materials with ordered pores, e.g., $C_2N$-*h*2D crystal and covalent organic framework (COF), have emerged.[14,15] Comparatively, conductive MOF-based materials possessing pores of narrow size distribution, tunable structure, and good electrical properties are expected to be another promising material for porous FETs.[16,17] To our knowledge, MOF-based FETs have never been reported.

In this work, microporous FET devices fabricated using a semiconductive MOF as the active channel were constructed. We highlight the preparation and characterization of a high-quality MOF membrane together with its fabrication and structure as well as the detailed characterization of the derived porous FETs. Notably, the FETs show a typical p-type depletion mode with the best on/off ratio of more than $10^3$ and field-effect charge mobility comparable to the best values obtained from devices based on solution-processed organic semiconductors or inorganic semiconductors.[18]

Among reported semiconductive MOFs, $Ni_3(HITP)_2$, which consists of nickel ions and organic HITP components (HITP = 2,3,6,7,10,11-hexaiminotriphenylenesemiquinonate), has drawn great attention for its interesting graphene-like honeycomb porous structure and excellent electronic conductivity (Figure 1a).[19] $Ni_3(HITP)_2$ membranes can be prepared by directly placing a quartz substrate inside the reaction vessel where the MOF is formed.[19] However, the obtained film is not compact and smooth. The challenge of preparing high-quality films has restricted the application of $Ni_3(HITP)_2$ in semiconductor devices. Herein we demonstrate an air–liquid interfacial method to prepare ultrasmooth and compact $Ni_3(HITP)_2$ membranes

**Received:** August 15, 2016
**Published:** October 30, 2016





DOI: 10.1021/jacs.6b08511
J. Am. Chem. Soc. 2017, 139, 1360–1363

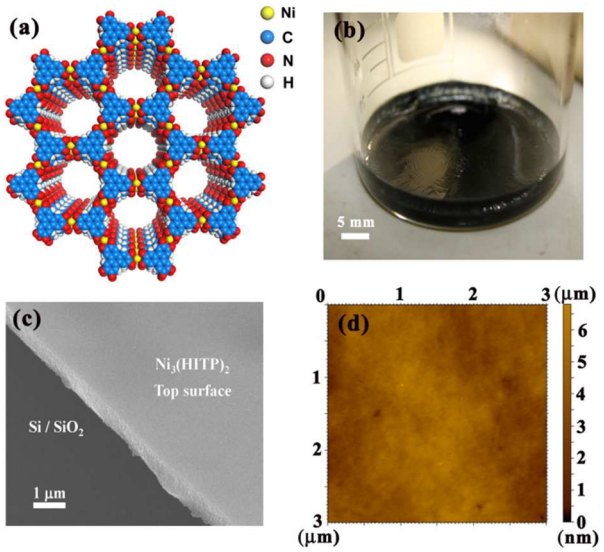


**Figure 1.** (a) Crystal structure of $Ni_3(HITP)_2$. (b) Photograph of a $Ni_3(HITP)_2$ membrane forming at the air−liquid interface. (c) SEM and (d) AFM images of the top surface of a $Ni_3(HITP)_2$ membrane.

for FET devices (for details, see the Supporting Information (SI)). Upon heating of an aqueous solution of HATP·6HCl (HATP = 2,3,6,7,10,11-hexaaminotriphenylene), $NiCl_2·6H_2O$, and trimethylamine to 60 °C (Scheme S1), $Ni^{2+}$ coordinates to in situ-generated HITP and self-assembles to form $Ni_3(HITP)_2$ nanoparticles at the air−liquid interface. The hydrophobic $Ni_3(HITP)_2$ nanoparticles float on the water surface, which acts as a "smooth substrate", and consequently the nanoparticles closely pack to form a nanometer-thick uniform layer due to the interface-confining effect (Figure S1).[20,21] After the air−liquid interface is fully covered with this $Ni_3(HITP)_2$ layer, the MOF membrane probably forms through continuous assembly of organic HITP components and nickel ions in the solution onto the $Ni_3(HITP)_2$ layer at the MOF−solution interface. The formation of the membrane at the interface could be observed even by the naked eye. The color of the membrane became deeper as the membrane grew thicker, and it finally turned dark blue-violet (Figure 1b). The thickness of the membrane was positively related to the reaction time, and a membrane with a thickness of ∼100 nm was obtained after reaction for 3 min.

In the structure of $Ni_3(HITP)_2$, the tritopic HITP moieties are connected by square-planar $Ni^{2+}$ centers to form a two-dimensional (2D) graphene-like honeycomb porous framework with sixfold symmetry (Figure 1a). In the lattice packing, two neighboring graphene-like layers stack in AB mode with an interval of 3.5 Å, resultin in 1D channels with an open window size of ∼1.4 nm. Figure S2 depicts the nitrogen sorption isotherms measured at 77 K, which show significant gas uptake and release during the adsorption and desorption processes. This observation indicates the permanent porosity in $Ni_3(HITP)_2$. The Brunauer−Emmett−Teller (BET) specific surface area and pore volume were calculated as 625 $m^2/g$ and 0.511 $cm^3/g$, respectively, which are comparable to values for other 2D crystalline porous materials.[22,23] To study the structure of the prepared $Ni_3(HITP)_2$ membrane, X-ray diffraction (XRD) patterns were further collected using two different scattering geometries: in-plane and out-of-plane (Figure S3). The prominent peaks in both the in-plane and out-of-plane XRD patterns at $2\theta = 4.7°$, 9.5°, 12.6°, 16.5°, and 27.3° are all present, which is consistent with the previously reported crystal structure of $Ni_3(HITP)_2$.[19] The in-plane and out-of-plane patterns have almost identical peaks, implying that the prepared membrane has no preferred orientation.

A $Ni_3(HITP)_2$ membrane was transferred onto a silicon wafer to evaluate its quality. Scanning electron microscopy (SEM) showed that the bottom surface of the prepared membrane at the air−liquid surface is relatively rough (Figure S4). However, the top surface of the same membrane is ultraflat, compact, and uniform on a large scale without any steps or cracks (Figure 1c). Atomic force microscopy (AFM) was used to further confirm the average surface roughness (RMS) of the top surface. As shown in Figure 1d, the top surface of the membrane was without pinholes and its RMS was only ∼1.05 nm over an area of 3 $\mu$m × 3 $\mu$m. Even over an area as large as 20 $\mu$m × 20 $\mu$m, the average RMS of nine randomly selected areas was only ∼1.43 nm (Figure S5). The high quality of the top surface of the solution-prepared membrane is comparable to those prepared by the vacuum deposition technique and good enough for FET device fabrication.

It is critical to know the composition of the thin layer (the top surface of the $Ni_3(HITP)_2$ membrane) close to the gate dielectric, which is where the majority of conduction occurs in a FET device. The XRD pattern of the top surface of the $Ni_3(HITP)_2$ membrane (Figure S3) shows no typical peaks of Ni, NiO, and $Ni(OH)_2$ (Figure S6). Meanwhile, the X-ray photoelectron spectroscopy (XPS) results (Figure S7) also revealed that the Ni $2p_{3/2}$ peak on the top surface of $Ni_3(HITP)_2$ membrane is located at 855.5 eV and has very weak broad satellite peak, which is the same as that of pure $Ni_3(HITP)_2$ crystallite in previous reports[19,24] but significantly different from those of Ni (852.6 eV), NiO (853.8 eV), and $Ni(OH)_2$ (855.2 eV)[25] (as analyzed in the SI). These observations rule out the presence of impurities of Ni species (e.g., Ni metal, NiO, and $Ni(OH)_2$) in the thin layer close to the $SiO_2$ layer.

As a class of newly emerging porous conducting materials, semiconductive MOFs are very attractive for use as active layers in FET devices to open their applications in electronic device fields and to develop new avenues for further revealing their electronic properties. Notably, a perfect semiconductor−dielectric interface is very important and necessary for a FET device.[26] The smooth and dense surface of the $Ni_3(HITP)_2$ membrane prepared in this work affords a great opportunity to prepare porous MOF−FET devices. As shown in Figure 2, we could easily transfer the as-prepared membrane to a $SiO_2$/Si wafer substrate in a top surface of membrane/$SiO_2$ mode by a simple stamping process. The smooth top surface of the $Ni_3(HITP)_2$ membrane directly contacts with the $SiO_2$/Si wafer, creating a high-quality interface between the MOF semiconductor and the $SiO_2$ dielectric. After deposition of patterned Au electrodes, porous FETs based on the MOF membrane were fabricated. Figures 2 and S8 show that the prepared device possessed a bottom-gate top-contact device geometry with a 105 nm thick membrane as the active channel material, 50 nm thick Au thin films as the source and drain electrodes, and heavily doped p-type Si as the gate electrode. The device has a channel length of 100 $\mu$m and a width of 1000 $\mu$m.

Figure 3a shows the output characteristics of the porous FET device. The drain−source current ($I_{ds}$) versus drain−source voltage ($V_{ds}$) curves of the device have good linear regimes, indicating good Ohmic contact between the Au electrodes and the porous $Ni_3(HITP)_2$ channel, which is favored for charge injection or exhaustion. They also show a gradual slope increase as the gate−source voltage ($V_{gs}$) decreases from 20 V to −20 V in


DOI: 10.1021/jacs.6b08511
J. Am. Chem. Soc. 2017, 139, 1360−1363

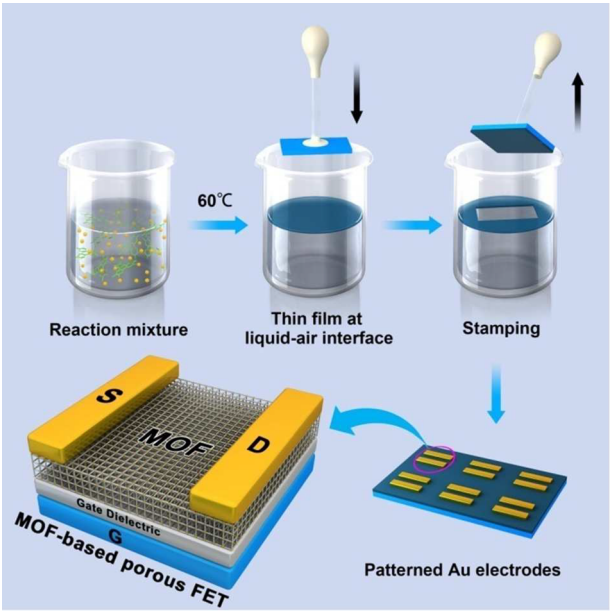


**Figure 2.** Fabrication of MOF-based porous FETs.

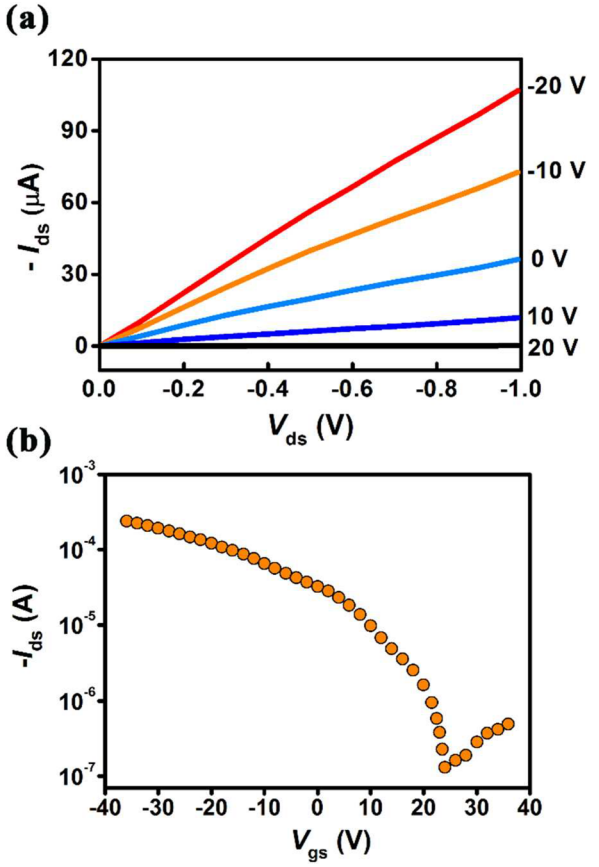


**Figure 3.** Electrical characteristics of $Ni_3(HITP)_2$-based FETs: (a) output curves; (b) transfer curves.

−10 V steps, which indicates that the carrier concentration in the porous channel can be effective modulated by altering $V_{gs}$. The conductivity of $Ni_3(HITP)_2$ in film form is 40 S·cm$^{-1}$ at room temperature,[19] but other electronic features, such as charge carrier type and charge mobility, have not been revealed. Figure 3b shows the transfer curve ($I_{ds}$ vs $V_{gs}$, with $V_{ds}$ = −1 V) of the porous FET device. The channel current gradually increases with decreasing $V_{gs}$, which confirms the observation in the output curves and also demonstrates that the device is a typical p-type transistor, where the application of a positive gate bias repels the carriers and a negative gate bias accumulates the carriers. The p-type behavior indicates that $Ni_3(HITP)_2$ is a semiconductor with holes as the majority carriers. The threshold voltage is ∼1.1 V, as extracted from the linear fit of $-I_{ds}$ versus $V_{gs}$ (Figure S9), which indicates that the device is a depletion-mode FET. Figure 3b also shows that the current on/off ratio in this device is approximately $2 \times 10^3$. Simultaneously, five other devices on the same $SiO_2$/Si substrate were also characterized (devices 2−6; Figure S10), and the current on/off ratios in these devices were between 350 and 2000 (Figure S11). The subthreshold swing (SS) value of this $Ni_3(HITP)_2$-based FET is 2.4 V/decade. The SS value in a FET depends on the number of defects in the interface between the active layer and the insulator layer.[27] The interface defect density ($N_t$) is $8.2 \times 10^{12}$ cm$^{-2}$ in this device, which indicates a relatively low defect density at the interface between the $Ni_3(HITP)_2$ channel layer and the $SiO_2$ gate dielectric. The high-quality interface in the porous FET is ascribed to the smooth surface of the free-standing $Ni_3(HITP)_2$ membrane. The calculated hole mobility was ∼48.6 cm$^2$ V$^{-1}$ s$^{-1}$ for this device and 38 ± 8 cm$^2$ V$^{-1}$ s$^{-1}$ for the five other devices (Figure S12), indicating excellent hole charge transport properties of the $Ni_3(HITP)_2$ membrane. The value surpasses those of most organic semiconductors and is even comparable to those of inorganic oxide semiconductors.[28] The reason for this high mobility might be elucidated from the point of view of the molecular structure of $Ni_3(HITP)_2$, where $Ni^{2+}$ coordinates to radical *o*-semiquinonate HITP to form an extended fully charge-delocalized layer in the *ab* plane of the crystal structure.[19] The $Ni(isq)_2$ (isq = *o*-diiminobenzosemiquinonate) part in the structure has been reported to show a rich electrochemical activity of reversible oxidation and reduction.[29] Therefore, charge carriers can transport within the layer smoothly. On the other hand, along the *c* axis of the structure, the above-mentioned conjugated layers overlap with an interval of only 3.5 Å, which is short enough to create sufficient orbital overlap between adjacent layers through $\pi-\pi$ interactions.[30] Thus, both the so-called "through-bond" channel (within the 2D layer) and "through-space" channel (between layers) for charge transport can be observed in $Ni_3(HITP)_2$ and may synergistically enhance the charge mobility in the membrane.[30] Notably, no transistor characteristic saturation was observed in our devices, and the on/off ratios of transfer curves were dramatically reduced with increasing $V_{ds}$ (Figure S13). This behavior may be attributed to the high conductivity of the $Ni_3(HITP)_2$ membrane. This phenomenon is common in FETs made from highly conductive channel materials like graphene and Cu−BHT.[31,32]

In conclusion, free-standing semiconductive porous membranes with a compact and smooth surface have been successfully prepared using an air−liquid interfacial self-assembly process. After they were transferred to $SiO_2$/Si substrates, the first microporous FETs with a MOF as the active channel material were demonstrated. The porous channel may greatly extend the applications of FETs to fields that require channel materials having large surface area and penetrability, such as FET-based sensors, voltage-gated ion channels, and microfluidic chips. The prepared FETs show distinguishable on and off states as well as a remarkably high charge mobility. Other electronic features of the MOF material, such as the charge carrier type and interface defect density, were also revealed for the first time by the FET


DOI: 10.1021/jacs.6b08511
J. Am. Chem. Soc. 2017, 139, 1360−1363

structure. Our results provide a step forward for both conductive MOF membranes and MOF-based devices. Moreover, the merits of MOFs, including variable and designable structure, regular pores, large surface areas, and band structure that is tunable by chemical modification, give us infinite imagination of its applications in electronic devices in the future.

## ■ ASSOCIATED CONTENT

### Supporting Information

The Supporting Information is available free of charge on the ACS Publications website at DOI: 10.1021/jacs.6b08511.

Experimental details and additional data (PDF)

## ■ AUTHOR INFORMATION


### Corresponding Authors

*junhe@gdut.edu.cn

*gxu@fjirsm.ac.cn

### Author Contributions

§G. Wu and J. Huang contributed equally.


### Notes

The authors declare no competing financial interest.

## ■ ACKNOWLEDGMENTS

This work was supported by the National Natural Science Foundation of China (51402293, 51602311), the Strategic Priority Research Program, CAS (XDB20000000), Fujian Natural Science Funds for Distinguished Young Scholar (2016J06006), Guangdong Natural Science Funds for Distinguished Young Scholar (15ZK0307), and the Fund for Returned Overseas Chinese Scholars Sponsored by the Ministry of Human Resources and Social Security of Fujian Province. We thank Prof. C. S. Li and Dr. J. S. Song for their help with the calculations.

## ■ REFERENCES


(1) Zhou, H. C.; Long, J. R.; Yaghi, O. M. *Chem. Rev.* **2012**, *112*, 673.

(2) (a) Chandler, B. D.; Enright, G. D.; Udachin, K. A.; Pawsey, S.; Ripmeester, J. A.; Cramb, D. T.; Shimizu, G. K. H. *Nat. Mater.* **2008**, *7*, 229. (b) Banerjee, R.; Phan, A.; Wang, B.; Knobler, C.; Furukawa, H.; O'Keeffe, M.; Yaghi, O. M. *Science* **2008**, *319*, 939. (c) Furukawa, H.; Cordova, K. E.; O'Keeffe, M.; Yaghi, O. M. *Science* **2013**, *341*, 1230444. (d) He, Y.; Zhou, W.; Qian, G.; Chen, B. *Chem. Soc. Rev.* **2014**, *43*, 5657. (e) Li, J. R.; Kuppler, R. J.; Zhou, H. C. *Chem. Soc. Rev.* **2009**, *38*, 1477.

(3) (a) Campbell, M. G.; Sheberla, D.; Liu, S. F.; Swager, T. M.; Dinca, M. *Angew. Chem., Int. Ed.* **2015**, *54*, 4349. (b) Kambe, T.; Sakamoto, R.; Hoshiko, K.; Takada, K.; Miyachi, M.; Ryu, J. H.; Sasaki, S.; Kim, J.; Nakazato, K.; Takata, M.; Nishihara, H. *J. Am. Chem. Soc.* **2013**, *135*, 2462. (c) Talin, A. A.; Centrone, A.; Ford, A. C.; Foster, M. E.; Stavila, V.; Haney, P.; Kinney, R. A.; Szalai, V.; El Gabaly, F.; Yoon, H. P.; Leonard, F.; Allendorf, M. D. *Science* **2014**, *343*, 66. (d) Kambe, T.; Sakamoto, R.; Kusamoto, T.; Pal, T.; Fukui, N.; Hoshiko, K.; Shimojima, T.; Wang, Z.; Hirahara, T.; Ishizaka, K.; Hasegawa, S.; Liu, F.; Nishihara, H. *J. Am. Chem. Soc.* **2014**, *136*, 14357. (e) Hmadeh, M.; Lu, Z.; Liu, Z.; Gándara, F.; Furukawa, H.; Wan, S.; Augustyn, V.; Chang, R.; Liao, L.; Zhou, F.; Perre, E.; Ozolins, V.; Suenaga, K.; Duan, X.; Dunn, B.; Yamamto, Y.; Terasaki, O.; Yaghi, O. M. *Chem. Mater.* **2012**, *24*, 3511.

(4) Erickson, K. J.; Leonard, F.; Stavila, V.; Foster, M. E.; Spataru, C. D.; Jones, R. E.; Foley, B. M.; Hopkins, P. E.; Allendorf, M. D.; Talin, A. A. *Adv. Mater.* **2015**, *27*, 3453.

(5) (a) Pan, L.; Ji, Z.; Yi, X.; Zhu, X.; Chen, X.; Shang, J.; Liu, G.; Li, R.-W. *Adv. Funct. Mater.* **2015**, *25*, 2677. (b) Yoon, S. M.; Warren, S. C.; Grzybowski, B. A. *Angew. Chem., Int. Ed.* **2014**, *53*, 4437.

(6) Campbell, M. G.; Liu, S. F.; Swager, T. M.; Dinca, M. *J. Am. Chem. Soc.* **2015**, *137*, 13780.

(7) Dacey, G. C.; Ross, I. M. *Bell Syst. Tech. J.* **1955**, *34*, 1149.

(8) (a) Guo, Y.; Yu, G.; Liu, Y. *Adv. Mater.* **2010**, *22*, 4427. (b) Gui, E. L.; Li, L. J.; Zhang, K.; Xu, Y.; Dong, X.; Ho, X.; Lee, P. S.; Kasim, J.; Shen, Z. X.; Rogers, J. A.; Mhaisalkar, S. G. *J. Am. Chem. Soc.* **2007**, *129*, 14427. (c) Mushrush, M.; Facchetti, A.; Lefenfeld, M.; Katz, H. E.; Marks, T. J. *J. Am. Chem. Soc.* **2003**, *125*, 9414. (d) Karnik, R.; Fan, R.; Yue, M.; Li, D. Y.; Yang, P. D.; Majumdar, A. *Nano Lett.* **2005**, *5*, 943.

(9) Zaumseil, J.; Sirringhaus, H. *Chem. Rev.* **2007**, *107*, 1296.

(10) Stavila, V.; Talin, A. A.; Allendorf, M. D. *Chem. Soc. Rev.* **2014**, *43*, 5994.

(11) (a) Phung, T.; Zhang, Y. L.; Dunlop, J.; Dalziel, J. *Biosens. Bioelectron.* **2011**, *26*, 3127. (b) Karnik, R.; Fan, R.; Yue, M.; Li, D. Y.; Yang, P. D.; Majumdar, A. *Nano Lett.* **2005**, *5*, 943. (c) Yu, C.; Davey, M. H.; Svec, F.; Frechet, J. M. J. *Anal. Chem.* **2001**, *73*, 5088. (d) Sainato, M.; Strambini, L. M.; Rella, S.; Mazzotta, E.; Barillaro, G. *ACS Appl. Mater. Interfaces* **2015**, *7*, 7136.

(12) Zan, H. W.; Dai, M. Z.; Hsu, T. Y.; Lin, H. C.; Meng, H. F.; Yang, Y. S. *IEEE Electron Device Lett.* **2011**, *32*, 1143.

(13) Lee, D. H.; Chang, Y. J.; Stickle, W.; Chang, C. H. *Electrochem. Solid-State Lett.* **2007**, *10*, K51.

(14) Mahmood, J.; Lee, E. K.; Jung, M.; Shin, D.; Jeon, I. Y.; Jung, S. M.; Choi, H. J.; Seo, J. M.; Bae, S. Y.; Sohn, S. D.; Park, N.; Oh, J. H.; Shin, H. J.; Baek, J. B. *Nat. Commun.* **2015**, *6*, 6486.

(15) Feldblyum, J. I.; McCreery, C. H.; Andrews, S. C.; Kurosawa, T.; Santos, E. J. G.; Duong, V.; Fang, L.; Ayzner, A. L.; Bao, Z. N. *Chem. Commun.* **2015**, *51*, 13894.

(16) Chen, B.; Xiang, S.; Qian, G. *Acc. Chem. Res.* **2010**, *43*, 1115.

(17) O'Keeffe, M.; Yaghi, O. M. *Chem. Rev.* **2012**, *112*, 675.

(18) (a) Dong, H. L.; Fu, X. L.; Liu, J.; Wang, Z. R.; Hu, W. P. *Adv. Mater.* **2013**, *25*, 6158. (b) Sun, H. B.; Wang, Q. J.; Qian, J.; Yin, Y.; Shi, Yi.; Li, Y. *Semicond. Sci. Technol.* **2015**, *30*, 054001. (c) Ahn, B. D.; Jeon, H.-J.; Sheng, J.; Park, J.; Park, J.-S. *Semicond. Sci. Technol.* **2015**, *30*, 064001. (d) Wang, Z. W.; Nayak, P. K.; Caraveo-Frescas, J. A.; Alshareef, H. N. *Adv. Mater.* **2016**, *28*, 3831.

(19) Sheberla, D.; Sun, L.; Blood-Forsythe, M. A.; Er, S.; Wade, C. R.; Brozek, C. K.; Aspuru-Guzik, A.; Dinca, M. *J. Am. Chem. Soc.* **2014**, *136*, 8859.

(20) Isz, S.; Weissbuch, I.; Kjaer, K.; Bouwman, W. G.; Als-Nielsen, J.; Palacin, S.; Ruaudel-Teixier, A.; Leiserowitz, L.; Lahav, M. *Chem. - Eur. J.* **1997**, *3*, 930.

(21) Rao, C. N.; Kalyanikutty, K. P. *Acc. Chem. Res.* **2008**, *41*, 489.

(22) Xu, G.; Otsubo, K.; Yamada, T.; Sakaida, S.; Kitagawa, H. *J. Am. Chem. Soc.* **2013**, *135*, 7438.

(23) DeBlase, C. R.; Silberstein, K. E.; Truong, T. T.; Abruna, H. D.; Dichtel, W. R. *J. Am. Chem. Soc.* **2013**, *135*, 16821.

(24) Miner, E. M.; Fukushima, T.; Sheberla, D.; Sun, L.; Surendranath, Y.; Dincă, M. *Nat. Commun.* **2016**, *7*, 10942.

(25) Grosvenor, A. P.; Biesinger, M. C.; Smart, R. S.; McIntyre, N. S. *Surf. Sci.* **2006**, *600*, 1771.

(26) Li, Y.; Liu, C.; Xu, Y.; Minari, T.; Darmawan, P.; Tsukagoshi, K. *Org. Electron.* **2012**, *13*, 815.

(27) Robertson, J. *Rep. Prog. Phys.* **2006**, *69*, 327.

(28) (a) Eda, G.; Chhowalla, M. *Adv. Mater.* **2010**, *22*, 2392. (b) Sirringhaus, H. *Adv. Mater.* **2014**, *26*, 1319. (c) Facchetti, A.; Yoon, M. H.; Marks, T. J. *Adv. Mater.* **2005**, *17*, 1705.

(29) Noro, S.; Chang, H. C.; Takenobu, T.; Murayama, Y.; Kanbara, T.; Aoyama, T.; Sassa, T.; Wada, T.; Tanaka, D.; Kitagawa, S.; Iwasa, Y.; Akutagawa, T.; Nakamura, T. *J. Am. Chem. Soc.* **2005**, *127*, 10012.

(30) Sun, L.; Campbell, M. G.; Dincă, M. *Angew. Chem., Int. Ed.* **2016**, *55*, 3566.

(31) Schwierz, F. *Nat. Nanotechnol.* **2010**, *5*, 487.

(32) Huang, X.; Sheng, P.; Tu, Z. Y.; Zhang, F. J.; Wang, J. H.; Geng, H.; Zou, Y.; Di, C. A.; Yi, Y. P.; Sun, Y. M.; Xu, W.; Zhu, D. B. *Nat. Commun.* **2015**, *6*, 7408.




DOI: 10.1021/jacs.6b08511
J. Am. Chem. Soc. 2017, 139, 1360−1363